Electrochemical and Thermodynamic Investigation of Nitrofurantoin as Effective Corrosion Inhibitor for Mild Steel in 1M Hydrochloric Acid Solution

Mareddy Jayanth Reddy[1], Chandra Bhan Verma[2], E E Ebenso[3], K K Singh[1], M A Quaraishi[2,]*

[1] Department of Metallurgical Engineering, Indian Institute of Technology, Banaras Hindu University, Varanasi 221005, India.
[2] Department of Chemistry, Indian Institute of Technology, Banaras Hindu University, Varanasi 221005, India.
[3] Material Science Innovation & Modelling (MaSIM) Focus Area, Faculty of Agriculture, Science and Technology, North-West University (Mafikeng Campus), Private Bag X2046, Mmabatho 2735, South Africa.
[*]E-mail: maquraishi.apc@itbhu.ac.in,maquraishi@rediffmail.com

In present study corrosion inhibition property of (E)-1-[(5-nitro-2furyl) methylideneamino] imidazolidine-2, 4-dione (Nitrofurantoin) in 1M HCl was investigated using weight loss, electrochemical impedance spectroscopy and potentiodynamic polarization, SEM and EDX techniques. From weight loss and electrochemical measurements it is observed that inhibition efficiency increases with Nitrofurantoin concentration and maximum efficiency (97.6) was obtained at 50 ppm. The potentiodynamic study reveals that Nitrofurantoin is a mixed type inhibitor. Adsorption of Nitrofurantoin on mild steel surface obeys the Langmuir adsorption isotherm. The morphology of the surface was examined by scanning electron microscopy (SEM), and the surface composition was evaluated using energy-dispersive X-ray spectroscopy (EDX) to verify the presence of Nitrofurantoin on the mild steel surface. The effect of temperature on the corrosion rate was investigated and some thermodynamic parameters were also calculated in order to explain the mechanism of adsorption.

1. INTRODUCTION

Mild steel is widely used as the constructional material in many industries due to its low cost and excellent mechanical properties. Mineral acids particularly hydrochloric acid is frequently used in

industrial processes during acid pickling, oil well acidizing, acid descaling, and acid cleaning due to its economical, efficient and trouble free properties [1-3]. The main problem of mild steel is its dissolution in acidic solutions. The damage by corrosion generates not only high cost for inspection, repairing and replacement, but in addition these constitute a public risk, thus the necessity of developing novel substances that behave like corrosion inhibitors especially in acid media [4]. Most of the commercial inhibitors are toxic in nature; there is a necessity for replacing them by environmentally friendly inhibitors [5-6]. The literature survey has revealed that the following drugs to be efficient corrosion inhibitors for corrosion in acidic solution: Metformin, Cefapirin, Cefuroxime, Doxycycline, Mebendazole, Ceftobiprole, Cefalexin, Dapsone, Ampicillin, Methocarbamol, Orphenadrine, Ketoconazole, Cefazolin, Cefotaxime, Abacavir, Acyclovir [7-19].

In our present work, inhibition property of Nitrofurantoin was investigated on mild steel in 1 M HCl using weight loss, electrochemical impedance, Tafel polarization techniques, Scanning Electron Microscopy, EDX. Nitrofurantoin is manufactured byMartin & Harris Laboratories pharmaceutical industry which consists of (E)-1-[(5-nitro-2furyl)methylideneamino]imidazolidine-2,4-dione. The chemical structure and IUPAC name is given in Figure 1.
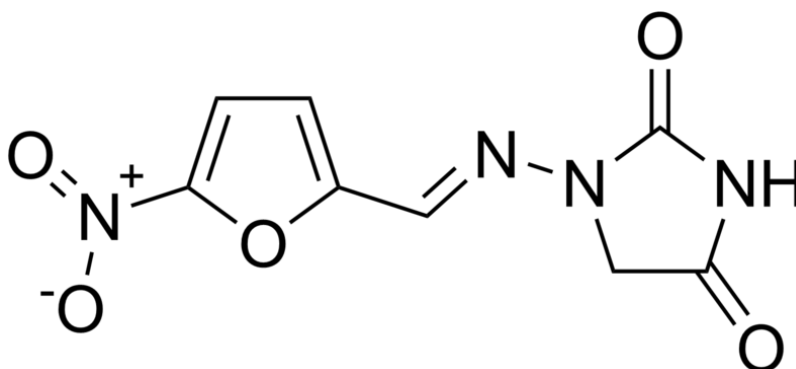
Figure 1. (E)-1-[(5-nitro-2furyl) methylideneamino]imidazolidine-2,4-dione.

2. EXPERIMENTAL

2.1 Material Preparation

The mild steel specimens having composition (wt %): C = 0.076, Mn = 0.192, P = 0.012, Si = 0.026, Cr = 0.050, Al = 0.023, and remainder Fe was used for weight loss and electrochemical measurements. Prior to experiment performed the mild steel specimens grinded and polished successively with emery papers from 600-1200 mesh/inch grade, washed in distilled water, degreased with acetone and finally dried in hot air blower. The samples were stored in desiccator before use. Weight loss experiments were conducted on mild steel specimens of dimension $2.5 \times 2.0 \times 0.025$ cm^3 and electrochemical measurements were conducted in 7.0 cm long stem (isolated with epoxy resin) to provide an exposed surface area 1.0 cm^{2}of working electrode (WE).

2.2 Test solution

The aggressive solution, 1 M HCl was used to carry out all weight loss and electrochemical experiments which was prepared by dilution of analytical grade 37% HCl with double distilled water.

2.3 Weight loss measurements

The mild steel specimens of having exposed area 2.5 cm X 2.0 cm x 0.025 cm was used for weight loss studies. The specimens are weighed accurately and then inserted in conical flasks containing 100 ml of 1 M HCl with and without Nitrofurantoin. After 3h immersion time mild steel specimens were taken out cleaned with water, dried and weighed accurately. All the experiments are performed in triplicate and mean value was reported. The inhibition efficiency (η %) and surface coverage (θ) were calculated at each concentration using following equation:

$$\eta\% = \frac{C_R - C_{R(i)}}{C_R} \times 100 \tag{1}$$

$$\theta = \frac{C_R - C_{R(i)}}{C_R} \tag{2}$$

where C_R and $C_{R(i)}$ are the corrosion rate values in absence and presence of Nitrofurantoin respectively. The corrosion rate (C_R) of mild steel in acidic medium was calculated by using following equation:

$$C_R = \frac{W}{At} \tag{3}$$

where, *W* is weight loss of mild steel specimens (mg), *A* is the area of the specimen (cm^2) and *t* is the exposure time (*h*).

2.4 Electrochemical impedance spectroscopy

The electrochemical experiments were carried out using a three electrode cell assembly with Gamry Potentiostat/Galvanostat having a Gamry framework system based on ESA400. In this three-electrode cell, mild steel specimens with exposed area 1.0 cm^2 as working electrode, a high purity platinum foil as counter electrode and saturated calomel electrode (*SCE*) as a reference electrode were used. All electrochemical potentials were measured versus *SCE* (saturated calomel electrode). Gamry applications include software EIS300 was used for all electrochemical impedance measurements. Echem Analyst version 5.50 software package was used for data fitting. It enables the fitting of the investigational results to a pure electronic model for representing the electrochemical system under investigation. Before performing electrochemical measurements the working electrode was immersed in 1 M HCl in absence and presence Nitrofurantoin for 30 minutes to stabilization of the *OCP w.r.t. SCE*. All the impendence measurements were performed under a potentiodynamic condition from 100,000 Hz to 0.01 Hz with amplitude of 10 mV peak-to-peak. The polarization measurements were

performed by changing the electrode potential automatically from -250 to +250mV vs. *OCP* at a scan rate of 1 mV s^{-1}. The linear Tafel segments of anodic and cathodic curves were extrapolated to obtain corrosion current densities (I_{corr}). From calculated corrosion current density inhibition efficiency calculated.

2.5 Surface Characterization

The mild steel specimens of size 2.5cm × 2 cm × 0.025 cm were immersed in 1 M HCl in absence and presence of optimum concentration (50 ppm)of Nitrofurantoin for 3 h immersion time. After elapsed time, the mild steel specimens were taken out, washed with distilled water, degreased with acetone, cleaned with absolute ethanol, dried and the surface examination were carried out at an accelerating voltage of 5 kV and 5K× magnification on a Ziess Evo 50 XVP instrument. Surface chemical composition of the corrosion products were recorded by an EDX detector coupled to the SEM.

3. RESULTS & DISCUSSIONS

3.1 Weight loss measurements

3.1.1 Effect of concentration
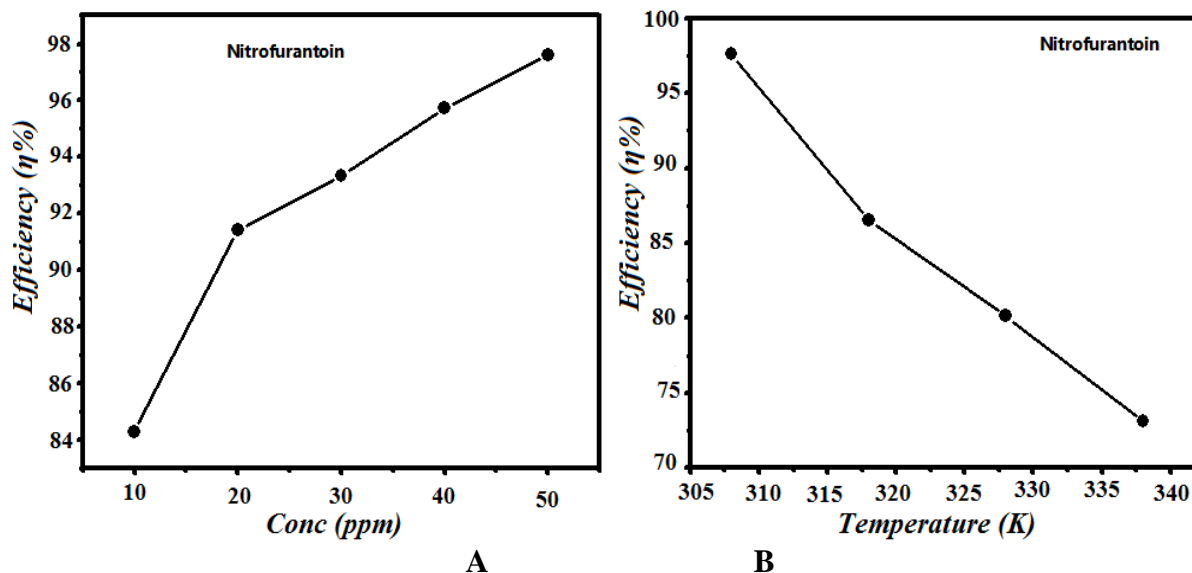
Figure 2. (a) Inhibition efficiency of Nitrofurantoin at different concentrations (b) Inhibition efficiency of Nitrofurantoin at different temperatures

The weight loss experiment conducted at various concentrations. The maximum inhibition efficiency for Nitrofurantoin was found at 50 ppm concentration. The variation of inhibition efficiency

with Nitrofurantoin concentration from 10 ppm to50 ppm is shown in Figure 2 (a).It is clear that on increasing Nitrofurantoin concentration inhibition efficiency increases. The values of percentage inhibition efficiency (η %), corrosion rate (C_R), Surface coverage (θ) and corresponding efficiency obtained from weight loss method at different concentrations are summarized in Table1.

Table 1. Corrosion rate and inhibition efficiency (**η %**) and surface coverage (**θ**) for the mild steel in 1 M HCl in the absence and in the presence of different concentration of Nitrofurantoin.

| Inhibitor	Inhibitor conc Ppm	Corrosion rate ($mg\ cm^{-2}\ h^{-1}$)	Surface coverage (θ)	Efficiency η%
No Inhibitor	--	7.60		
Nitrofurantoin	10	1.13	0.8428	84.28
	20	0.62	0.9142	91.42
	30	0.46	0.9333	93.33
	40	0.33	0.9571	95.71
	50	0.16	0.9761	97.61

3.1.2. Effect of Temperature:

To show the effect of temperature on inhibition efficiency of Nitrofurantoin, weight loss experiment was performed in the temperature range of 308- 338 K at optimum concentration of Nitrofurantoin. The variation of inhibition efficiency with temperature at optimum concentration of Nitrofurantoin is shown in Figure 2(b). From Figure 2(b), it is clear that corrosion rate is temperature dependent and increases with increasing the temperature. This decrease in inhibition is due to desorption of inhibitors from metal surface [20].Thus, at higher temperature , more desorption of inhibitor molecules takes place and larger surface area of metal come in contact with acid, resulting in an increase in corrosion rate [21].The values of percentage inhibition efficiency (η %), corrosion rate (C_R), Surface coverage (θ) and corresponding efficiency obtained from weight loss method at different concentrations are summarized in Table2.

Table 2. Corrosion rate, inhibition efficiency (**η %**) and surface coverage (**θ**) for the mild steel in 1 M HCl in the absence and in the presence of optimum concentration of Nitrofurantoin at different temperature.

Inhibitor	Temperature (K)	Corrosion rate ($mg\ cm^{-2}\ h^{-1}$) Blank	Corrosion rate ($mg\ cm^{-2}\ h^{-1}$) Inhibitor	Surface coverage (θ)	η%
Nitrofurantoin (50 ppm)	308	7.6	0.166	0.97	97.619
	318	9.66	1.33	0.86	86.551
	328	14.6	2.91	0.80	80.136
	338	18.7	5.03	0.73	73.131

3.1.3 Thermodynamic parameters and adsorption isotherm
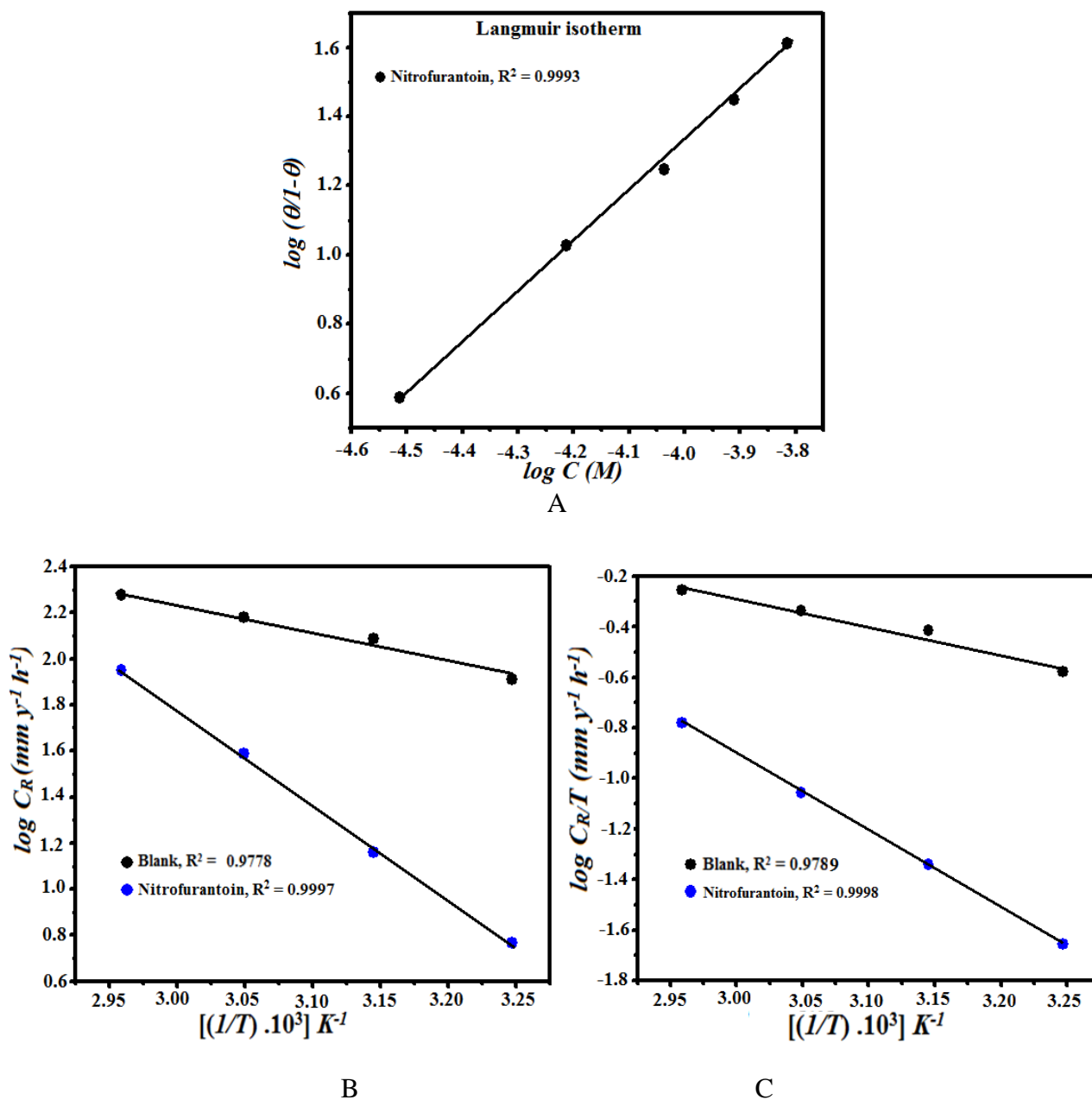
Figure 3. (a) Langmuir adsorption isotherm, (b) Arrhenius plots of log C_R versus $1/T$ (c) Transition state plots of log C_R/T versus $1/T$

Different adsorption isotherms were tested in order to obtain more information about the interaction between the Nitrofurantoin and the mild steel surface. Various isotherms were tested, including Temkin ($R^2 = 0.9850$), Frumkin ($R^2 = 0.9370$) and Langmuir ($R^2 = 0.9993$) adsorption isotherms. Langmuir adsorption isotherm was found to be best fit which assumes that the solid surface contains a fixed number of adsorption sites and each site holds one adsorbed species [22]. Langmuir isotherm gives a straight line between log ($\theta/1-\theta$) and log C (M) as shown below in Figure 3 (a).

The corrosion rate (C_R) depends upon temperature and this temperature dependence corrosion rate of a chemical reaction can be expressed by following Arrhenius and transition state equation [23].

$$\log(C_R) = \frac{-E_a}{2.303RT} + \log \lambda \tag{4}$$

$$C_R = \frac{RT}{Nh} \exp\left(\frac{\Delta S^*}{R}\right) \exp\left(-\frac{\Delta H^*}{RT}\right) \tag{5}$$

where E_a is activation energy for the corrosion of Mild Steel in 1 M HCl, λ pre-exponential factor, R is the gas constant, A the Arrhenius pre-exponential factor and T is the absolute, h is Plank'^{s} constant, N is Avogadro's number, ΔS^* is the entropy of activation and ΔH^* is the enthalpy of activation temperature.

The Arrhenius plot for mild steel immersed in 1M HCl in inhibitor-free and with inhibitor solution is depicted in Figure 3(b). The plot obtained was straight lines and apparent activation energies (E_a) at optimum concentration of inhibitors were determined by linear regression between log C_R vs. 1/T and listed in Table2. All the linear regression coefficients are close to unity. Inspection ofTable2 reveals that E_a values are higher in presence of Nitrofurantoin than in absence of Nitrofurantoin. The increase in E_a may be either due to physical adsorption in first stage [24-27] or due to decrease in the adsorption of inhibitor molecules on the mild steel surface with increase in temperature [28]. The increase in value of E_a in the presence of Nitrofurantoin may also be due to increase thickness of the double layer which retards the corrosion process [29].

Figure 3 (c) represents the plot between log C_R/T vs. 1/T which give a straight lines from their gradient ((ΔH^* = -slope/2.303R) and intercept (log(R/Nh) + ($\Delta S^*/$ 2.303R)]) of which values of the ΔH^* and ΔS were calculated and given in Table3.Study of Table 3 reveals that the value of ΔH^* for dissolution of mild steel in 1M HCl in presence of Nitrofurantoin is higher (66.78 kJ mol^{-1}) than that in absence of Nitrofurantoin(26.04 kJ mol^{-1}).The positive sign and higher value of ΔH^*reflected the endothermic nature of mild steel dissolution process, which mean that dissolution of mild steel is in presence of Nitrofurantoin is difficult [30].The shift towards positive value of entropies (ΔS^*) shows that the activated complex in the rate determining step represents dissociation rather than association, meaning that disordering increases on going from reactants to the activated complex[31].

The standard free energy of adsorption, ΔG^o_{ads} and the values of equilibrium constant, K_{ads} at different temperatures is calculated from the equation [32].

$$\frac{C_{(inh)}}{\theta} = \frac{1}{K_{(ads)}} + C_{(inh)} \tag{6}$$

$$\Delta G^o_{ads} = -RT \ln(55.5 K_{ads}) \tag{7}$$

Generally, the value of $\Delta G^o_{ads} \leq -20$ kJ mol^{-1} signify physisorption and values more negative than -40 kJ mol^{-1} signify chemisorption [33]. For investigated drug the calculated values of ΔG^o_{ads} is -30.10 KJ mol^{-1} suggesting that adsorption of Nitrofurantoin on mild steel surface involves both physical as well as chemical adsorption [34-35].

Table 3. Thermodynamic parameters for mild steel in 1M HCl in absence and presence of optimum
concentration of Nitrofurantoin.

Inhibitor	E_a(kJ mol^{-1})	ΔH (kJ mol^{-1})	ΔS (J K^{-1} mol^{-1})	ΔG(kJ mol^{-1})
Blank	28.48	26.04	-148.9	....
Nitrofurantoin	64.43	66.78	-13.28	-30.10

3.2.1. Potentiodynamic polarization measurements

Polarization measurements were carried out in order to gain knowledge regarding the kinetics of the cathodic and anodic reactions polarization curves of the mild steel electrode in 1M HCl in absence and at different concentrations of inhibitor and is shown in Figure 4.
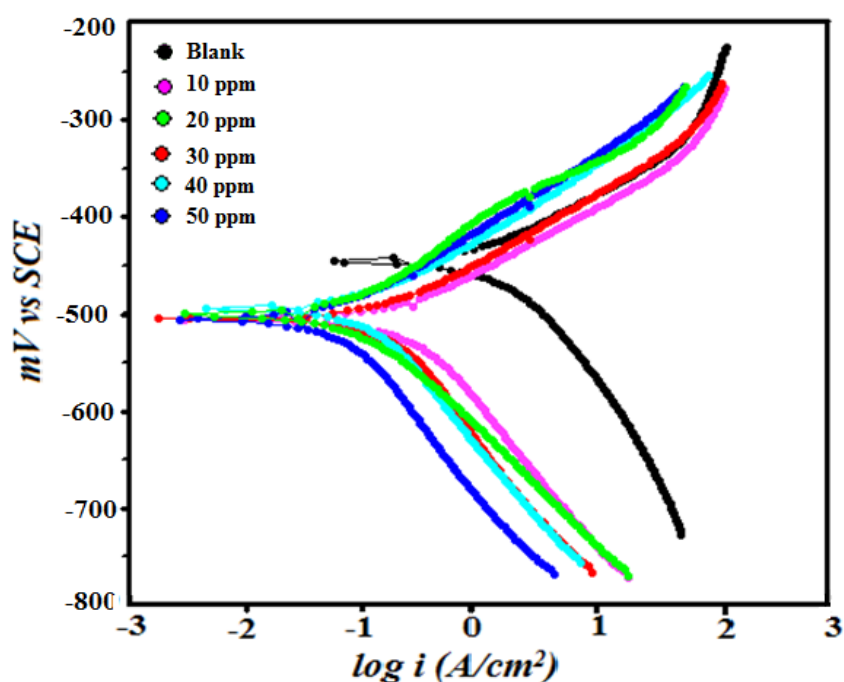
Figure 4. Tafel polarization curves for corrosion of mild steel in 1.0 M HCl in the absence and presence of different concentrations of Nitrofurantoin.

In the presence of inhibitor molecules, the anodic and cathodic current decreased and the effect rises with increasing concentration. Reduction in anodic dissolution of mild steel with inhibitor addition, along with retarded hydrogen evolution attributes to the adsorption of inhibitor on active metal sites present on mild steel surface [36].By extrapolating the linear segments of cathodic and anodic Tafel lines, values of corrosion potential (E_{corr}) and corrosion current density ($Icorr$)were calculated. From calculated corrosion current density, inhibition efficiency was derived using following equation:

$$\eta\% = \left(1 - \frac{I_{\text{corr(i)}}}{I_{\text{corr}}}\right) \times 100 \qquad (8)$$

Where $I_{corr\,(i)}$ and I_{corr} are corrosion current density without and with presence of Nitrofurantoin, respectively. Various potentiodynamic parameters such as corrosion potential (Ecorr), corrosion current densities (Icorr), anodic Tafel slopes (β_a), cathodic Tafel slopes (β_c), inhibition efficiency and corresponding surface coverage were calculated tabulated in Table 6. In literature, it has been reported that (i) if the displacement in E_{corr} is >85 *mV* of inhibitor with respect to E_{corr} of blank acid solution, the inhibitor could be recognized as cathodic or anodic type and (ii) if displacement in E_{corr} is < 85, the inhibitor can be considered as mixed type[37]. The inspection of the Table4 reveals that Ecorr value does not change significantly in presence of Nitrofurantoin suggesting that it is a mixed type inhibitor.

Table 4. The Potentiodynamic polarization and linear polarization parameters and corresponding efficiencies of Nitrofurantoin in 1.0 M HCl at different concentration

| *Tafel data*								*Linear Polarization data*		
Inhibitor	Conc ppm	I_{corr} µA/cm^2	E_{corr} mV/SCE	β_a mV/dec	β_c mV/dec	θ	$\eta\%$	R_{p}	θ	$\eta\%$
Blank	0.0	1150	-445	75	124.6	….	-4.5454	12.3	….	….
	10	207	-501	89.2	101.3	0.8118	81.181	69.35	0.8226	82.26
	20	136.5	-494	80.7	173.2	0.8759	87.590	137.5	0.9105	91.05
Nitrofurantoin	30	83.56	-501	89.2	101.8	0.9240	92.403	178.9	0.9312	93.12
	40	53.47	-505	81.5	160.5	0.9513	95.139	263.5	0.9525	95.25
	50	37.23	-504	75.8	169.8	0.9661	96.615	298.3	0.9587	95.87

3.2.2 LPR (Linear Polarization Resistance)

Polarization resistance (R_p) was calculated from linear segment of the linear polarization curves in vicinity to corrosion potential. From calculated polarization resistance corrosion inhibition efficiencies and corresponding surface coverage were calculated and given in Table4. It is observed that inhibition efficiencies increase with increasing the concentration of Nitrofurantoin which is in good agreement with results obtained from weight loss, EIS data and potentiodynamic measurements.

3.2.3 Electrochemical Impedance Spectroscopy

Impedance method provides information about the kinetics of the electrode processes and simultaneously about the surface properties of the investigated systems. The shape of impedance gives mechanistic information. The corrosion behavior of mild steel in 1 M HCl in absence an presence of different concentrations of Nitrofurantoin were investigated by EIS after immersion for 30 min at 303 ± 1 K. Nyquist and Bode plots of mild steel in uninhibited and inhibited acid solutions containing optimum concentrations of Nitrofurantoin are presented in Figure 5 (a) and (b).
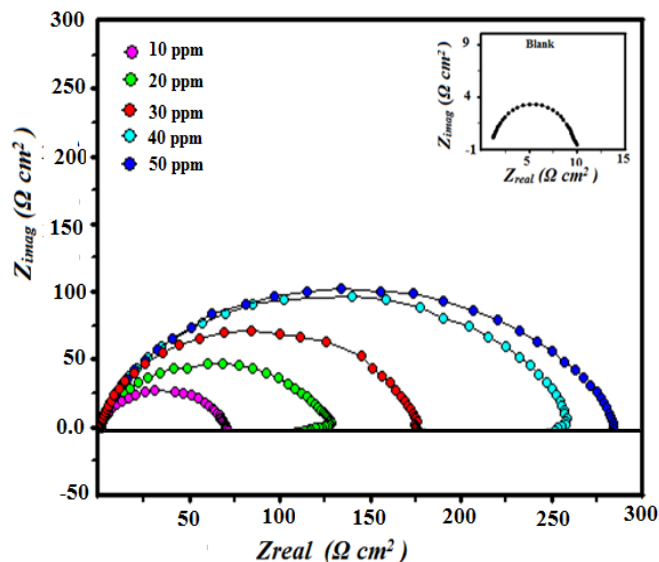
A
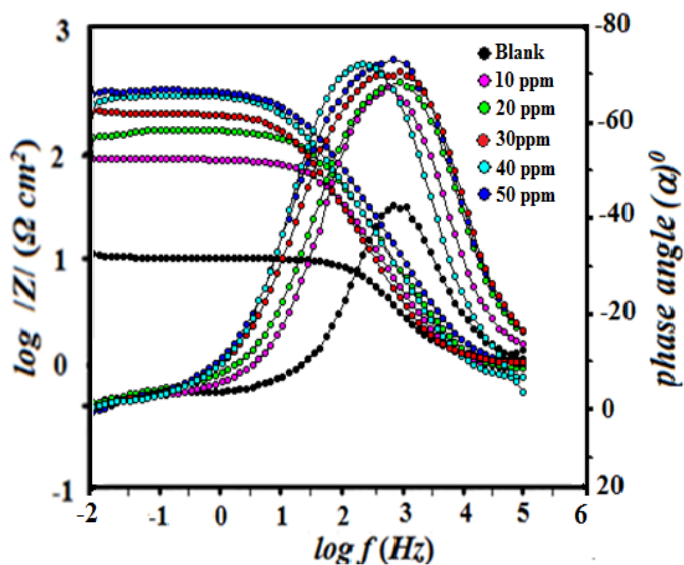
B
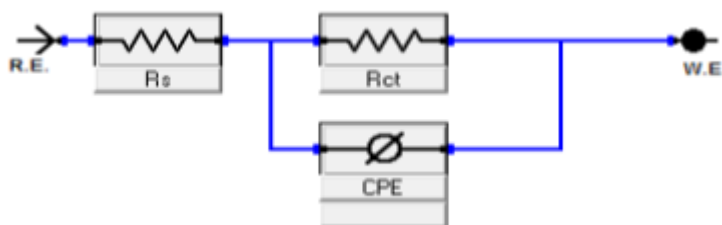
C

Figure 5. (a) Nyquist plot in absence and presence of optimum concentrations of Nitrofurantoin (b)Bode plot in absence and presence of optimum concentrations of Nitrofurantoin (c)Equivalent circuit used to fit the data

The Nyquist plots show a depressed capacitive loop shifted along the real impedance (Zre axis) axis in the high frequency (HF) range and an inductive loop in the lower frequency (LF) range (in Bode plot). The HF capacitive loop can be attributed to the charge transfer reaction and time constant of the electric double layer and to the surface non-homogeneity of structural or interfacial origin, such as those found in adsorption processes [38]. The LF inductive loop may be attributed to the relaxation of adsorbed compound on electrode surface [39-40]. It has been observed that diameter of semicircular loop increases with increase Nitrofurantoin concentrations. The increasing diameter of capacitive loop obtained in 1 M HCl in presence of Nitrofurantoin indicated the inhibition of corrosion of mild steel. The EIS parameters for Nitrofurantoin such as R_s, Y_0, R_{ct} and C_{dl} were derived from the Nyquist plot are given in Table4.

It is apparent from Table 5 that the impedance of the inhibited system amplified with increasing the Nitrofurantoin concentrations and the C_{dl} values decreased with increasing Nitrofurantoin concentrations. The double layer capacitance (C_{dl}) was calculated by using following equation [41]:

$$C_{dl} = Y_0 \, (\omega_{max})^{n-1} \qquad\qquad (9)$$

where, Y_0 is *CPE* coefficient, n is *CPE* exponent (phase shift), ω is the angular frequency. The ω_{max} represents the frequency at which the imaginary component reaches a maximum. This decrease in C_{dl} results from a decrease in local dielectric constant and/or an increase in the thickness of the double layer, suggested that Nitrofurantoin molecules inhibit the iron corrosion by adsorption at the metal/acid interface [42].The depression in Nyquist semicircles is a feature for solid electrodes and often referred to as frequency dispersion and attributed to the roughness and other in homogeneities of the solid electrode [43]. It is worth noting that the percentage inhibition efficiencies obtained from impedance measurements are comparable and run parallel with those obtained from weight loss and potentiodynamic polarization measurements.

Table 5. The Electrochemical Impedance parameters and corresponding efficiencies of Nitrofurantoin in 1.0 M HCl at different concentration

| Inhibitor	Conc. (ppm)	R_s (Ω)	R_{ct} ($\Omega\ cm^2$)	N	Y_0 ($\mu F\ cm^{-2}$)	C_{dl} (μFcm^{-2})	$\square$	$\eta\%$
Blank	0.0	1.12	11.8	0.827	249.8	106.21	….	….
	10	1.13	62.83	0.868	96.31	53.72849	0.805	80.51727
	20	0.941	124.05	0.844	82.3	38.55771	0.901	90.1322
	30	1.183	172.417	0.893	65.7	36.01624	0.929	92.90035
Nitrofurantoin	40	0.782	252.818	0.856	72.56	34.81826	0.951	95.15818
	50	1.036	276.264	0.846	61.4	34.61351	0.955	95.56909

Figure 5 (b) represent the Bode impedance magnitude and phase angle plots recorded for mild steel electrode immersed in 1 M HCl in the absence and presence of Nitrofurantoin at its open circuit potential. It is clear from Figure 5 (b) that the log |Z| values and phase angle fall to zero at high frequency region. A linear relationship between log |Z| vs log f with a slope near −1 and the phase

angle nearly −70° at around intermediate frequency region, has been observed. This is a characteristic response of capacitive behavior at intermediate frequencies. The deviation from ideal capacitive behavior (slope = -1 and phase angle = 90^0) [44] these deviations were considered to be the deviation from the ideal capacitive behavior at intermediate frequencies. The Bode phase angle plots exhibit one time constant (single maximum) at intermediate frequencies, and broadening of this maximum in the presence of Nitrofurantoin accounts for the formation of a protective layer on the electrode surface [45].

4. SURFACE INVESTIGATION

4.1 SEM Analysis.

SEM micrographs obtained for mild steel surface after three hours immersion time in absence and presence of optimum concentration (50 ppm) of Nitrofurantoin are shown in Figure 6 (a-b). A comparison can be drawn with the surface morphology of the micrographs. Figure 6 (a) shows the mild steel surface micrograph in uninhibited solution which reveals a very rough surface with cracks and pits due to rapid corrosion attack; it can be concluded that mild steel surface was greatly damaged in absence of Nitrofurantoin. Figure 6 (b) is the morphology that resulted after testing in 1 M HCl in the presence of Nitrofurantoin the results proved that there is less damage on steel surfaces and the Nitrofurantoin can protect mild steel surface effectively in 1 M HCl, which is due to strong adsorption of the inhibitor on metal surface to suppress the corrosion.
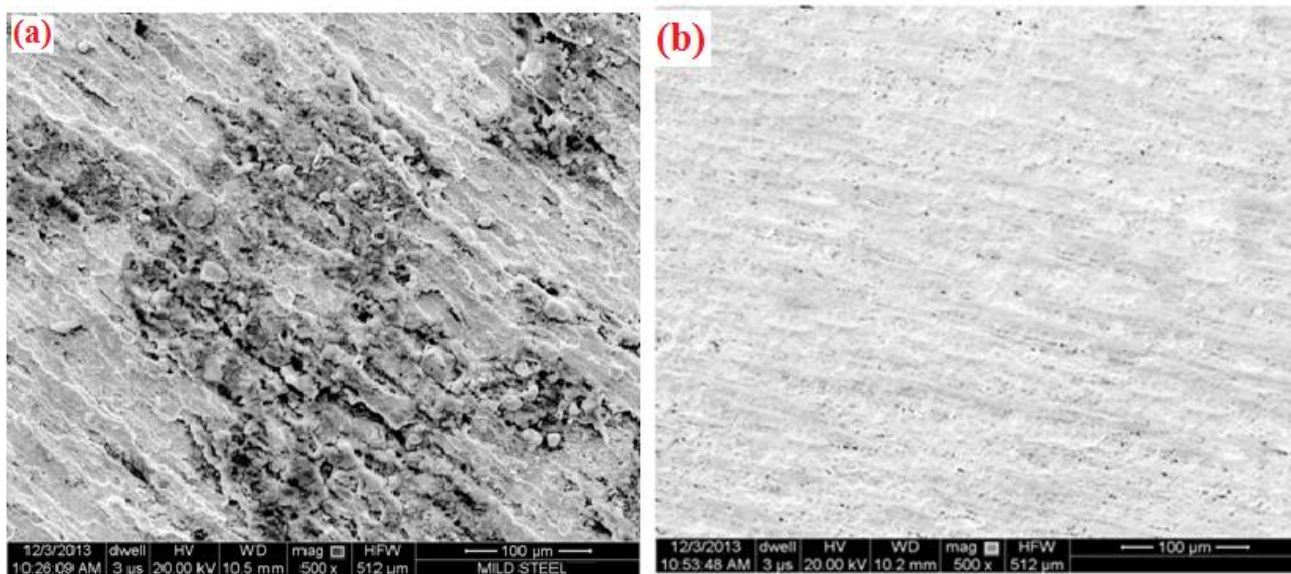
Figure 6. (a) Surface of mild steel in the absence of inhibitor (b) Surface of mild steel in presence of inhibitor

4.2. EDX Analysis.

The EDX examinations of the mild steel surfaces were performed in 1 M HCl solution in absence and presence of optimum concentration of Nitrofurantoin. The EDX survey spectra were used to determine the elements present on mild steel surface. To achieve our goal, mild steel surface composition examined before and after exposure to the inhibitor solution. The percentage atomic content of mild steel samples obtained from EDX analysis is listed in Table6.

Table 6. Percentage atomic contents of elements obtained from EDX spectrum of Nitrofurantoin

Inhibitor	Fe	C	N	O
Blank	63.09	36.10	-----	-----
Nitrofurantoin	63.22	23.24	5.53	6.89

The results of EDX survey spectra are displayed in Figure 7 (a-b). Figure 7 (a) represent the EDX spectrum of mild steel in absence of Nitrofurantoin. The EDX spectrum of uninhibited mild steel specimen, the peak of O and N are absent which confirms the dissolution of air-formed oxide film and free corrosion of bare metal. However, for inhibited solutions the EDX spectra [Figure 7 (b)] showed additional lines characteristic for the existence of N and O (due to the N and O atoms of the Nitrofurantoin).
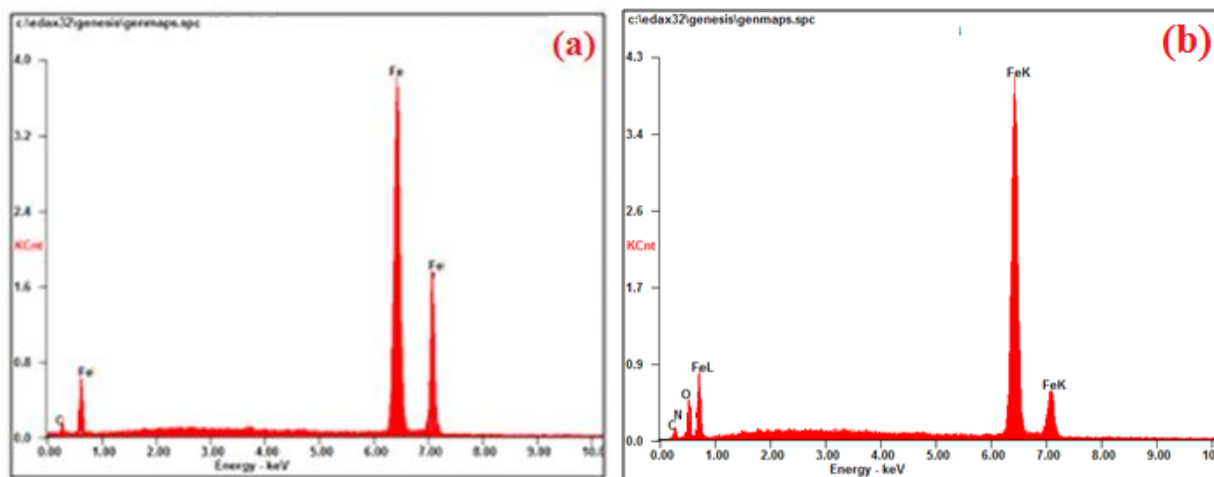
Figure 7. (a) EDX of mild steel in the absence of inhibitor (b) EDX of mild steel in presence of inhibitor

5. MECHANISM OF INHIBITION

Corrosion inhibition of mild steel in 1M HCl by Nitrofurantoin can be explained on the basis of molecular adsorption. It is generally considered that the first step in the corrosion inhibition of a metal

is the adsorption of the inhibitors molecules at metal / solution interface [46]. The Nitrofurantoin can adsorb on the mild steel surface by following ways: (a) Electrostatic interaction between the charged molecules and charged metal; (b) Interaction of π-electrons with the metal; (c) Interaction of unshared pair of electrons in the molecule with the metal; and (d) The combination of the all the effects [47-49]. Concerning inhibitors, the inhibition efficiency depends on several factors; such as the number of adsorption sites and their charge density, molecular size, heat of hydrogenation, mode of interaction with the metal surface and the formation metallic complexes

The adsorption of Nitrofurantoin cannot be considers as purely physical or purely chemical phenomenon. The charge on metal surface is due to electric field which emerges at the metal/electrolyte interface. It is well-known that mild steel specimens are positively charged with respect to the potential of zero charge (*PZC*) in acid solutions [50]. It is a well-known fact that the inhibitors not only offer electrons to metal atoms but also have unoccupied higher energy orbital to accept electrons from d-orbital of metal atom for strengthening of bonding interaction [51-52].

In aqueous solution of 1M HCl Nitrofurantoin molecule may adsorb through protonated heteroatoms and already adsorbed Cl^- on mild steel surface. Initially, the protonated form of Nitrofurantoin molecules in acid medium start competing with H^+ ions for electrons on mild steel surface. After release of H_2 gas, the cationic form of inhibitors returns to its neutral form and heteroatoms with free lone pair electrons promote chemical adsorption. Thus, there is a synergism between the adsorbed Cl^- ions and protonated Nitrofurantoin. Hence, we can assume that the inhibition of mild steel corrosion in 1 M HCl is due to the adsorption of Nitrofurantoin on the mild steel surface.

6. CONCLUSIONS

From above study it is concluded that:
1.   Nitrofurantoin is good corrosion inhibitors for corrosion of mild steel in 1M HCl solution. The maximum efficiency was found to be 97% at 50 ppm concentration.
2.   The adsorption of Nitrofurantoin molecule on mild steel surface obeyed the Langmuir isotherm.
3.   The Potentiodynamic studies reveal that Nitrofurantoin is a mixed type inhibitors i.e. it affected both cathodic and anodic reactions.
4.   The negative values of ΔG shows that adsorption of Nitrofurantoin on mild steel is a spontaneous process.
5.   The results obtained from weight loss and electrochemical methods are in good agreement.

References

1. M.A. Quraishi, R. Sardar, *Corrosion* 58 (2002) 748.
2. S.A. Abd El-Maksoud, A.S. Fouda, *Mater. Chem. Phys*. 93 (2005) 84.
3. M.A. Migahed, I.F. Nassar, *Electrochim. Acta*53 (2008) 2877.
4. G. Trabanelli, *Corrosion* 47 (1991) 410.

5.   P.B. Raja, M.G. Sethuraman, *Mater. Lett.* 62 (2008) 113.
6.   G. Broussard, O. Bramantit, F.M. Marchese, *O Occup. Med.* 47 (1997) 337.
7.   A.K. Singh, M. A. Quraishi and Eno E. Ebenso, *Int. J. Electrochem. Sci.,* 6 (2011) 5676.
8.   S. K. Shukla and M. A. Quraishi, *Corros. Sci.* 52 (2010) 314.
9.   I. Ahamad M. A. Quraishi, *Corros. Sci.* 52 (2010), 651.
10. A. K. Singh M. A. Quraishi. *Journal of Applied Electrochem.* 41 (2011) 7.
11. S. K. Shukla and M. A. Quraishi, *Mater. Chem. Phys.* 120 (2010) 142
12. A. Singh, A. K. Singh and M. A. Quraishi, *the Open Electrochem. J.* 2 (2010) 43.
13. N. O. Eddy, Eno E. Ebenso and U. J. Ibok, *J. Appl. Electrochem.* 40 (2010) 445.
14. I. B. Obot, *Port. Electrochim. Acta.* 27 (2009) 539.
15. E E. Ebenso, N. O. Eddy and A. O. Odiongenyi, *Port. Electrochim. Acta.* 27 (2009) 13
16. N. O. Eddy, U. J. Ibok, Eno E. Ebenso, A. El Nemr and E.S.H. El Ashry, *J. Mol. Mod.* 15 (2009) 1085.
17. A. K. Singh and M. A. Quraishi, *Corros. Sci.* 52 (2010) 152.
18. S. K. Shukla and M. A. Quraishi, *Corros. Sci.* 51(2009) 1007.
19. C Verma, M.A. Quraishi, E.E. Ebenso *Int. J. Electrochem. Sci.,* 8 (2013) 7401 .
20. I. Ahamad, R. Prasad and M.A. Quraishi, *Corros. Sci.* 52 (2010) 3033.
21. Sudheer, M.A.Quraishi, *Corros. Sci.* 70 (2013) 161.
22. A.O. Yuce, R. Solmazb, G. Kardas, *Mater. Chem. Phys.* 131 (2012) 615 -620.
23. I. Ahamad, R. Prasad, M.A. Quraishi (2010) *Corros. Sci.* 52 1472– 1481.
24. E.A. Noor, A.H. Al-Moubaraki, *Mater. Chem. Phys.* 110 (2008) 145–154.
25. L. Larabi, Y. Harek, O. Benali, S. Ghalem, *Prog. Org. Coat.* 54 (2005) 256–262.
26. L. Larabi, O. Benali, Y. Harek, *Mater. Lett.* 61 (2007) 3287–3291.
27. T. Szauer, A. Brandt, *Electrochim. Acta* 26 (1981) 1209–1217.
28. C.S. Venkatachalam, S.R. Rajagopalan, M.V.C. Sastry, *Electrochim. Acta* 26 (1981) 1219–1224.
29. A.O. Yuce, G. Kardas, *Corros. Sci.* 58 (2012) 86 -94.
30. N.M. Guan, L. Xueming, L. Fei, *Mater. Chem. Phys.* 86 (2004) 59–68.
31. M.A. Quraishi, A. Singh, V.K. Singh, D.K. Yadav, A.K.singh, *Mater. Chem. Phys.,* 122   (2010) 114.
32. I. Ahamad, R. Prasad, M.A. Quraishi, *Corros. Sci.* 52 (2010) 1472.
33. A. M. Fekry, R. R. Mohamed, *Electrochim. Acta*, 55 (2010) 1933.
34. A. Doner, R. Solmaz, M. Ozcan, G. Kardas *Corros. Sci.* 53 (2011) 2902.
35. P.R. Roberge (2000) Handbook of Corrosion Engineering, *McGraw-Hill, New York.*
36. M.A. Quraishi, S. Ahmad, G. Venkatachari, *Bull. Electrochem.* 12 (1996) 109.
37. O. Riggs, L.Jr. Corrosion Inhibitors, 2nd ed.; C. C. Nathan (1973) Houston, *TX, USA*; p 109.
38. R.S. Goncalves, D.S. Azambuja, A.M. SerpaLucho, *Corros. Sci.* 44 (2002) 467.
39. M.A. Amin, S.S. Abd El-Rehim, E.E.F. El-Sherbini, R.S. Bayyomi, *Electrochim.Acta* 52 (2007) 3588.
40. M.A. Veloz, I. Gonzalez, *Electrochim. Acta* 48 (10) (2002) 135.
41. C. S. Hsu and F. Mansfeld, *Corrosion* 57 (2001) 747
42. A Sorkhabi, D. Seifzadeh, M.G. Hosseini, *Corros. Sci.* 50 (2008) 3363.
43. A. Popova, M. Christov, Corros. Sci. 48 (2006) 3208.
44. E. Naderi, A. H. Jafari, M. Ehteshamzadeha, M. G., Hosseini, *Mater. Chem. Phys.* 115 (2009) 852
45. H. H. Hassan, *Electrochim. Acta* 53 (2007) 1722.
46. M. Sahin, S. Bilgic, H. Yilmaz, *Appl. Surf. Sci.*, 195 (2002) 1.
47. D.P. Schweinsberg, G.A. George, A.K. Nanayakkara, D.A. Steiner, *Corros. Sci.* 28 (1988) 33.
48. H. Shorky, M. Yuasa, I. Sekine, R.M. Issa, H.Y. El-Baradie, G.K. Gomma, *Corros. Sci.* 40 (1998) 2173.
49. A.K. Singh, M.A. Quraishi, *Corros. Sci.* 52 (2010) 152.
50. S. Deng, X. Li, H. Fu *Corros. Sci*, 53(2011)760.

51. R.S. Goncalves, D.S. Azambuja, A.M. SerpaLucho, *Corros. Sci.* 44 (2002) 467.
52. G.N. Mu, T.P. Zhao, M. Liu, T. Gu, *Corros.* 52 (1996) 853.